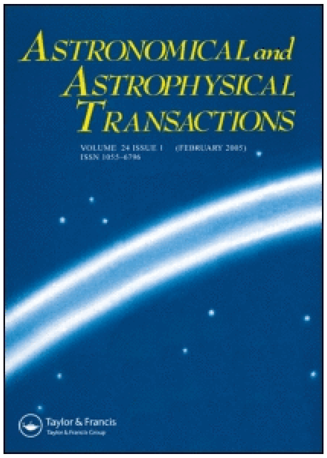

Astronomical & Astrophysical Transactions
The Journal of the Eurasian Astronomical Society
Publication details, including instructions for authors and subscription information:
http://www.informaworld.com/smpp/title~content=t713453505

Space-time distributions of the coronal green-line brightness and solar magnetic fields

O. G. Badalyan [a]; V. N. Obridko [a]; J. Sýkora [b]
[a] Institute of Terrestrial Magnetism, Ionosphere and Radio Wave Propagation, Troitsk, Russia
[b] Astronomical Institute of the Slovak Academy of Sciences, Tatranská Lomnica, Slovak Republic

Online Publication Date: 01 December 2004
To cite this Article: Badalyan, O. G., Obridko, V. N. and Sýkora, J. (2004) 'Space-time distributions of the coronal green-line brightness and solar magnetic fields', Astronomical & Astrophysical Transactions, 23:6, 555 - 566
To link to this article: DOI: 10.1080/10556790412331335336
URL: http://dx.doi.org/10.1080/10556790412331335336

Astronomical and Astrophysical Transactions
2004, Vol. 23, No. 6, pp. 555–566

SPACE–TIME DISTRIBUTIONS OF THE CORONAL GREEN-LINE BRIGHTNESS AND SOLAR MAGNETIC FIELDS

O. G. BADALYAN[a,*], V. N. OBRIDKO[a] and J. SÝKORA[b]

[a]*Institute of Terrestrial Magnetism, Ionosphere and Radio Wave Propagation, 142190 Troitsk, Russia*
[b]*Astronomical Institute of the Slovak Academy of Sciences, 05960 Tatranská Lomnica, Slovak Republic*

(Received 24 November 2004)

The space-time distribution of brightness of the Fe XIV, 530.3 nm coronal green line and its cyclic variations are analysed for a long time interval of more than five cycles (1943–2001). For this purpose a special movie has been made. It is shown that a substantial spatial reorganization of the coronal green-line brightness (CGLB) takes a relatively short time and occurs close to the so-called reference points of the cycle, as derived from the series of various solar activity indices. The 'active longitudes' lasting for 1.5–3.0 years are found to exist in the CGLB. The antipodal and 'intermittent' active longitudes are identified. For the time interval 1977–2001, it has been corroborated that the CGLB is strongly influenced by the magnetic field strength. An agreement is shown to exist between the spatial structure on the CGLB synoptic charts and those of the magnetic field strength. It is shown that the nature of the relationship between the CGLB and the magnetic field strengths in the corona inside and outside the sunspot formation zone differ significantly.

KEYWORDS: Sun, corona, coronal green line, cyclic variations, coronal magnetic field

1 INTRODUCTION

The intensity of the brightest emission line (Fe XIV, 530.3 nm) of the optical solar corona is a very informative index of solar activity. Nowadays, quite a long set of systematic measurements of the coronal green line brightness (CGLB) is available, covering more than five solar activity cycles. A specific advantage of this index results from its almost simultaneous registration at all solar latitudes. This allows the solar activity to be studied all over the Sun by uniform data, contrary, for example, to the Wolf numbers characterizing activity at lower latitudes only, and the polar faculae appearing at high latitudes.

The coronal green line (CGL) originates in the inner corona at a temperature of about 2 MK, most favourable for generation of the Fe XIV ion. Since the CGL intensity is proportional to the square of electron density, regions of the strongest CGL emission are mostly identical with dense loops and loop clusters in the inner corona. Such structures are related to and controlled by the coronal magnetic fields. Therefore, a proper analysis of the CGLB space–time distribution permits us to investigate some aspects of the coronal magnetic field evolution.

* Corresponding author. Email: badalyan@izmiran.troitsk.ru

ISSN 1055-6796 print; ISSN 1476-3540 online
DOI: 10.1080/10556790412331335336

It should be emphasized that the CGLB is measured directly, while the strength and structure of the coronal magnetic fields are extrapolated from the photospheric measurements and calculated under the specific simplifying assumptions. In addition, the period covered by the CGLB measurements substantially exceeds the period of accessible photospheric magnetic field data.

Comparison of the CGLB space–time distribution with the magnetic field parameters seems to be a promising method to analyse the solar activity variations and mechanisms of the coronal heating. It should be noted, however, that there are a few papers only in which the data on the CGL emission are directly compared with the magnetic measurements. Guhathakurta *et al.* (1993) performed a comparison of the coronal brightness with the magnetic field data for the period 1984–1992. They compared the calculated coronal temperature with the distribution of the white-light corona and the line-of-sight component of the magnetic field at the photosphere measured at Kitt Peak Observatory. The coronal temperature was calculated from the intensity ratio of the red (Fe X, 637.4 nm) and green (Fe XIV, 530.3 nm) lines. Note that this method is dubious since the lines in question form in different regions in the corona. The above workers were aware of these doubts, as seen from their later work (Guhathakurta *et al.* 1996). The temperature distribution obtained by Guhathakurta *et al.* (1993) is hardly like that of the magnetic field.

For the present paper, it is more interesting to discuss the space–time distributions of the green-line and red-line corona brightness as presented by Guhathakurta *et al.* (1993). They found that the distribution of the CGLB is rather similar to that of the magnetic field. At the ascending phase of the cycle, one can see midlatitude zones of the increased brightness in both solar hemispheres. As the cycle maximum approaches, these bands expand to both higher and lower latitudes, while a single equatorial zone is formed close to the cycle minimum.

Another way of comparing the CGLB with the magnetic field parameters was applied by Wang *et al.* (1997). They analysed SOHO LASCO C1 images taken on 4 days with characteristic green-line structures. Measurements at the Wilcox Solar Observatory (Stanford University) were used to calculate the structure of the magnetic field lines assuming the potential approximation. The magnetic field structures and the CGLB distribution proved to agree perfectly well. It was shown that the density at the feet of the magnetic tubes and the magnetic field strength were related by the expression $n_{\rm foot} \propto \langle B_{\rm foot}\rangle^{0.9}$.

The corona images obtained with the Yohkoh, SOHO, TRACE and CORONAS facilities cover the period since 1991. These observations allow comparison the images taken in different lines in the extreme ultraviolet and X-ray lines with the daily maps of the observed magnetic field. The λ-195 Å, Fe XII emission originates virtually in the same regions where the CGL does. The images taken at $\lambda = 195$ Å show that the coronal emission is enhanced over the active regions and is attenuated over the coronal holes. However, since the types of equipment on different space missions are not identical, the observational data may lack uniformity. This circumstance as well as a relatively small period of extra-atmospheric observations, reduce the possibility of using these data for the study of long-lasting and cyclic variations in physical conditions in the inner corona.

Long-lasting patrol observations of the CGLB are useful also when investigating the persistent problem of the so-called ‘active longitudes’ (ALs). Long series of data are required to study this phenomenon. In the past, various indices of solar activity have been used by a number of workers (Vitinsky *et al.*, 1986a; Stewart and Bravo, 1996; Bumba *et al.*, 2000; Neugebauer *et al.*, 2000; Berdyugina and Usoskin, 2003). It should be noted, however, that these results are considerably controversial for various reasons. Firstly, the rotation velocity of various tracers proved to differ from the Carrington rotation (CR). Moreover, it was shown that the solar plasma transporting the tracers might occasionally manifest two rotation angular velocities. Secondly, it is well known that the rotation velocity depends on latitude, and this dependence is likely to be different for various tracers. Finally, the tracer method is inherently deficient since the tracers do not form a continuous numerical field. Thus, to obtain such a field from, for example, sunspots, we must take into account their occurrence frequency at a given point on the solar surface. However, above the latitude of 30° the sunspots are very rare and the reliability of the result decreases. Therefore, a real advantage of the CGLB for AL studies is in providing a uniform and continuous numerical field everywhere on the disc over a long time scale. Investigation of the ALs by using the CGLB data over shorter time intervals were performed by Benevolenskaya *et al.* (2000) and Xanthakis *et al.* (1991, 1996).

Let us give a basic characterization of our CGLB database. The patrol coronagraphic measurements, regularly carried out by a small worldwide network of observatories, were synthesized to create the photometrically homogeneous database of the Fe XIV, 530.3 nm coronal emission line intensities (for details, see Sýkora (1971, 1992), Badalyan, *et al.* (2001b) and Sýkora and Rýbak (2004)). The data from different observatories were reduced to the height of 60″ and the space resolution of the measurements is 1 day in the solar longitude (approximately 13°) and 5° in the solar latitude. Originally, the measurements were available from both the east and west solar limbs. From these, central meridian (CM) data were derived as an average of intensities measured 7 days before and 7 days later, that is as an average of values when the proper meridian passed the east and west limbs, correspondingly. At the same time, the original position angles were transformed to the solar latitudes. Subsequently, the CM data were used to construct all the figures in this paper. The CGLB database covers the 1943–2001 period and can be time analysed at individual solar latitudes, over arbitrary latitudinal zones, separately in the north and south solar hemispheres, and/or a daily index of the coronal activity of the Sun as a star can be derived. The time-latitude variations and periodicity in the CGLB were studied by Sýkora (1980, 1992, 1994) and Sýkora *et al.*(2002).

In the present paper, the CGLB space–time distributions are investigated for 18–23 solar cycles. A set of the synoptic charts averaged over six CRs allows us to look for cyclic variations in the CGLB spatial distribution, to reveal the presence of the ALs and to trace their evolution, and to identify the intermittent antipodal ALs. Comparison of the CGLB synoptic charts with those of the coronal magnetic field strength makes it possible to establish a degree of mutual correspondence of both phenomena and to study the relationship between the cyclic variations in the CGLB and the coronal magnetic fields. This is a way to study the large-scale evolutionary relationships of the magnetic field and CGLB based on the long data series that we have at our disposal. Such an approach could reveal the effect of the magnetic fields of various scales on the physical conditions in the corona.

In order to analyse the cyclic variation in the CGLB distribution, we prepared a special movie visualizing our database for the time interval from 1943 to 2001. The movie allowed us to reveal typical features and evolution in the CGLB distribution and to identify the moments of relatively fast restructuring of the green-line corona. Our movie is accessible at http://helios.izmiran.rssi. ru/hellab/Badalyan/green/, together with the coloured figures of the present paper.[†]

2 CYCLIC VARIATIONS IN THE SPATIAL DISTRIBUTION OF THE CORONAL GREEN-LINE BRIGHTNESS

The cyclic variations and evolution of the CGLB spatial distribution were mainly investigated by constructing the individual CGLB synoptic charts, each of which represents data averaged

[†]The CD-ROM movie is available on request.

over six subsequent CRs. Smoothing over six CRs was applied to identify, first of all, the long-lived and relatively large-scale features. Finally, the movie was assembled from the whole set (784 frames) of the averaged synoptic charts. The frames of the movie show the coronal brightness in conventional colouring.

The movie covers the period under investigation (cycles 18–22 and part of cycle 23). Since each frame represents the averaging over six CRs the time identification of the individual frames corresponds to the middle of the six-CR time interval, that is to the beginning of the fourth CR. At the same time, the shift between the adjacent frames is one CR. An eight-level CGLB gradation is adopted in the frames, the maximum brightness being displayed by yellow and the minimum brightness by cyan. The maximum brightness was chosen individually for each frame (see below).

The moments of typical reorganizations of the general CGLB distribution are more apparent from the inspection of a longer sequences of synoptic charts. Therefore, to identify these moments, we considered it useful to analyse special plane-table maps, each of which are composed of about 15–20 frames (as, for example, in Figure 2 shown later).

Such reorganizations were compared with the reference points of the solar cycle derived from a set of the solar activity indices, basically, from sunspot numbers (Vitinsky *et al.*, 1986b; Kuklin *et al.*, 1990; Obridko and Kuklin, 1994; Kuklin and Obridko, 1995; Obridko and Shelting, 2003). These points manifest fundamental changes in the space–time organization of solar activity rather than a mere jump of the time derivative of any index. The concept of reference points seems to be essential for understanding the nature of solar activity and its prediction. Their simplified meaning is as follows: t_{mA} and t_{AM} are the beginning and the end respectively of the ascending phase of the cycle, and t_{MI} and t_{Dm} represent the beginning and the end respectively of the descending phase. Also the points m and M indicating the minimum and maximum respectively of the activity cycle are added to the reference points.

Figure 1 illustrates evolution of the CGLB distribution over solar cycle 21, as an example. A particular range of brightness from zero to $I_{\max}$ is applied for each chart in this figure; the darker shading corresponds to the higher brightness while white denotes the minimum brightness. In order to visualize better the transition from minimum to maximum of the cycle, the step in ΔI has been brought into a certain accord with the cyclic variation in CGLB. Thus, in fact, each chart has its own scaling. The maximum number of grey grades on one chart is 8; however, some of the charts (*e.g.* charts 1, 2 and 6 in Figure 1) are actually less graded. The real values of ΔI are given within the rectangles to the right of the charts, together with the years and corresponding reference points. The year indicated corresponds approximately to the centre of the averaged six CRs. Note that, in the synoptic charts of this figure (and all figures below), time increases from right to left.

One can see the following evolution of the CGLB during solar cycles. At the cycle minimum, the CGLB is weak all over the Sun, only several isolated and slightly brightened regions being observed. Two ‘rivers’ with a few separate brightened ‘islands’ inside them appear close to the t_{mA} reference point (beginning of the ascending branch of the cycle). Approaching t_{AM} (end of the ascending phase), the ‘rivers’ become stable and substantially brighter. At the cycle maximum M, the ‘rivers’ begin to join and touch one another, while at t_{MD} (beginning of the descending branch) they form one flow with two well-pronounced streams. Finally, to the end of the descending phase (t_{Dm}), one relatively narrow equatorial ‘river’ is formed and it begins to disintegrate into the individual ‘islands’ of brightening. A similar evolution can be demonstrated for all five solar cycles under examination.

Some more details of the space–time CGLB evolution may be perhaps better understood if we examine a set of the successive synoptic charts. Figure 2 shows evolution of the large-scale coronal structuring during the descending phase of cycle 21. Similarly to Figure 1, each chart represents the CGLB distribution averaged over six CRs. Here, successive charts

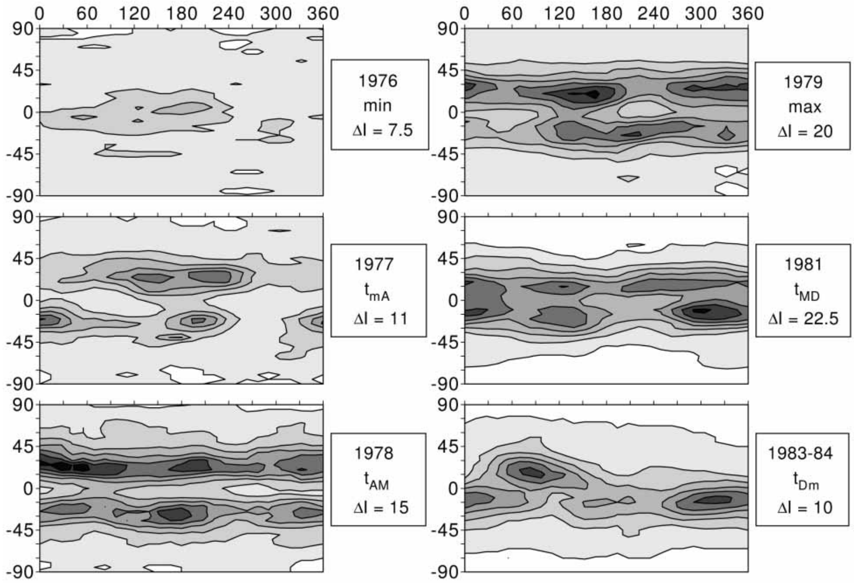

Figure 1. Characteristic CGLB synoptic charts for cycle 21. Each of the charts represents the data averaged over six CRs. Darker shading corresponds to the greater brightness while, the white areas stand for the lowest brightness. The ΔI step (different for each chart) is in absolute coronal units (acu) and given within the rectangles to the right of the charts. The corresponding year and reference point are indicated for each synoptic chart also. The heliographic longitude and latitude are on the abscissa and ordinate axes respectively. The time increases from right to left on all the synoptic charts of this and the following figures.

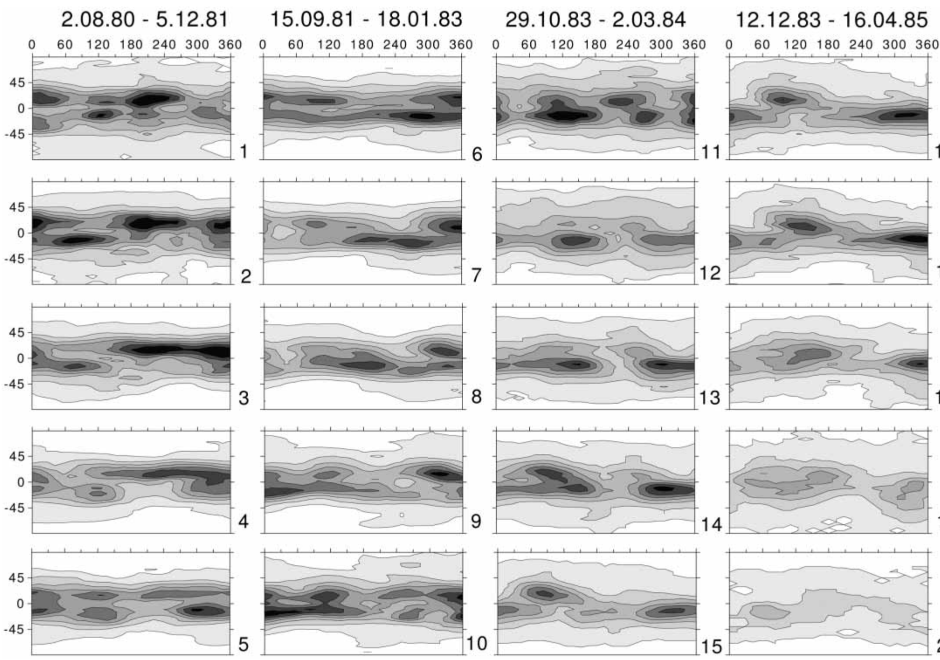

Figure 2. A series of synoptic charts covering the descending phase of cycle 21. Each chart represents the CGLB distribution averaged over six CRs with an interval of three CRs between the neighbouring charts. The numbers to the right of each chart denote the time sequence along the columns. The step ΔI in the charts is successively equal to 20, 20, 22.5, 22.5, 22.5, 20, 20, 17.5, 16.25, 15, 11.25, 11.25, 11.25, 10, 10, 8.75, 8.75, 7.5, 5 and 5 acu.

are separated by an interval of three CRs. Gradual changes in the brightness distribution and a permanent existence of the active longitudes (1.5–3.0 years in duration) are visible. For example, on the charts 1–5, a strengthening of brightness is noticeable at a longitude of about 210°, shifting successively to 240°. Over this period, the AL is more distinct in the northern hemisphere. Later (charts 6 and 7), the brightening in the above-mentioned longitudinal interval is better pronounced in the southern hemisphere and gradually disappears. On the contrary, in chart 12 and the following charts, a certain ‘valley’ (decrease in brightness) is apparent at those longitudes. Quite often, two bright enhancements can be identified at approximately the same longitudes in the northern and southern hemispheres (*e.g.* charts 10, 11 and 14) as one complex region existing synchronously in both hemispheres. Approaching the solar minimum, a general decrease in CGLB is clearly seen in the corresponding charts.

Table 1 presents the moments of the CGLB spatial reorganization as determined from the scenario of the CGLB cyclic variations described above. The first column gives the number of the activity cycle. The left-hand columns for each reference point give the CR when the CGLB reorganization occured while, in the right-hand columns, the CR related to the reference points determined from the Wolf numbers and large-scale magnetic fields are presented (Obridko and Shelting, 2003). In some cases, the moments of the reference points determined from the Wolf numbers and those determined from the large-scale magnetic fields (especially for t_{mA}) do not coincide. In these cases, the table provides two values. Moreover, there are three cases when we were unable to determine unambiguously the reference points (the moments of reorganization) also from the CGLB.

It should be noted that, when introducing a concept of the reference points, Vitinsky *et al.* (1986b) suggested that the dates of the reference points determined by different solar indices should coincide. In most cases, this is true. However, determining the exact dates of reference points is a rather complicated task. It requires as much information as possible, and the use of data on the solar corona might be very promising.

Figure 3 represents nine annual latitude–time charts of solar cycle 21. Two ‘rivers’ and their evolution are well displayed in these charts also. In the ascending phase of the cycle, one can readily see the 27 and 13 day periods in the CGLB distribution. This means that two antipodal ALs (*i.e.* longitudes differing by 180°) do exist almost synchronously on both solar hemispheres. During 1982, at the beginning of the descending phase, the 27 day period is easily recognizable in the shape of the outer envelope isoline. At the equatorial latitudes, the 13 day period is permanently present. On approaching 1984, the bright regions begin to penetrate from one to another solar hemisphere. This behaviour, which is particularly well pronounced in 1984, resembles something like ‘intermittent’ ALs. This means that the ALs in the northern and southern hemispheres are activated alternately. Finally, in 1985 only the 27 day period in CGLB is observed in the equatorial zone, which means that only one AL is present on the Sun.

Table 1. Moments of spatial reorganizations of CGLB distribution.

Cycle	t_{mA}		t_{AM}		M		t_{MD}		t_{Dm}	
18	1230	1229	1244	1242	1251	1256	1276	1282	1313	1306
19	1360	1363	1376	1379	1390	1393	1424	1419	1444	1440
20	1497, 1514	1499, 1519	1525	1520, 1529	1540	1540	1560	1558	1596	1598, 1615
21	1657	1656, 1665	1677	1680	1684	1692	1698, 1714	1715	1749	1759, 1748
22	1791	1781, 1804	1815	1812	1820	1818	1834	1840	1877	1875
23	1924	1929, 1940	1954	1955	1956	1961				

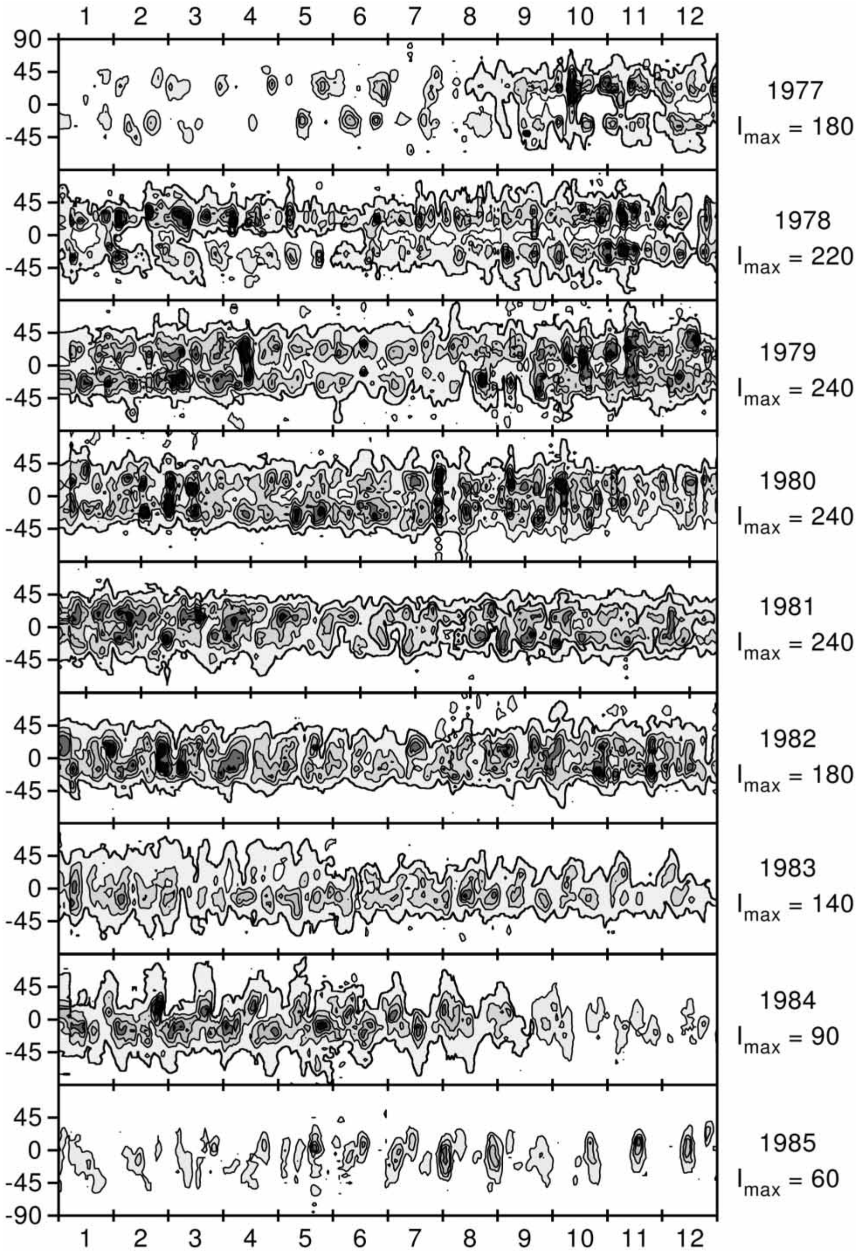

Figure 3. **A series of the annual time–latitude charts for cycle 21. The entire brightness range is divided into six levels. The years and the maximum brightnesses are listed to the right of each chart. The months of the year are given on the abscissa axis.**

The possibility of the quantitative description of the space–time CGLB evolution by applying principal component analysis was proposed by Badalyan and Kuklin (1993, 2000). Badalyan *et al.* (2001a) developed this idea further and applied it to the database under consideration. The papers by Badalyan and Kuklin (2000) and Badalyan *et al.* (2001a), as well as some additional comments on the principal component analysis application are available at the website http://helios.izmiran.rssi.ru/hellab/Badalyan/.

3 GLOBAL STRUCTURING OF THE CORONAL GREEN-LINE BRIGHTNESS AND CORONAL MAGNETIC FIELD

The magnetic field strength B in the corona was calculated from the Wilcox Solar Observatory photospheric measurements (the data were obtained via the Internet) under the potential approximation. The value of B was calculated using $B = (B_r^2 + B_t^2)^{1/2}$, where B_r and B_t are the radial and tangential components respectively. The synoptic charts of the total magnetic field strength are derived for a distance of $1.1R_{.}$ and averaged over six CRs, similarly to the CGLB charts.

Figure 4 represents three pairs of synoptic charts for the magnetic field strength (upper charts) and the CGLB (lower charts); the darker regions denoting higher values of the corresponding parameter. One can see quite good agreement between the general structures for each pair of the charts. For example, both the CGLB and the magnetic field strength evidently increase during the period 13 January 1981–24 July 1981 at longitudes of about 200° and 320°, particularly in the northern hemisphere. In the period from 11 April 1983 to 21 September 1983, the most characteristic features are the decrease in both parameters at longitudes close to 180–200° and their increase on both sides of this longitudinal interval. During the period 12 December 1983–23 May 1984, a region of enhancement is particularly well pronounced at longitudes of 70–130° in the northern hemisphere, while the magnitudes of both parameters in the southern hemisphere are considerably reduced at those longitudes. Therefore, a conclusion on the generally positive correlation between the CGLB and the coronal magnetic field strength in the sunspot formation zone seems to be reasonable. To a great extent, this is because the dense compact structures of the enhanced CGLB are formed by magnetic fields of relatively high intensity.

To demonstrate such a relation also quantitatively, we calculated the correlation coefficients between the corresponding points of the CGLB and magnetic field synoptic charts. The calculation was performed separately for the entire latitude range ±70°, and for individual latitudinal zones. The details of the calculation have been described by Badalyan and Obridko (2004a, b). The results for the maps presented in Figure 4 are given in Table 2. The correlation

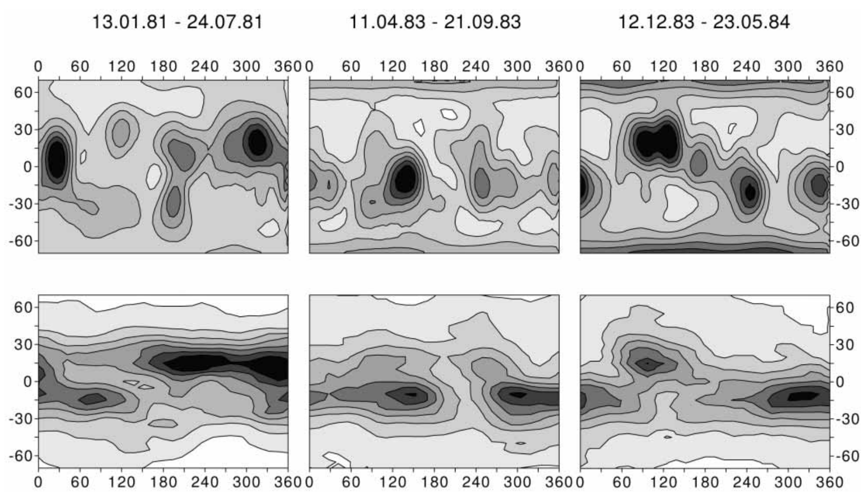

Figure 4. **Comparison of three pairs of synoptic charts created for the magnetic field strength (upper charts) and CGLB (lower charts). The total magnetic field strength was derived for a distance of 1.1$R_{.}$. Similar to Figure 1, each chart represents the data averaged over six CRs; the corresponding time intervals are indicated at the top.**

Table 2. Correlation coefficients between the CGLB and the magnetic field strength.

		Correlation coefficient		
CR	*Time interval*	±70°	±30°	$\|\varphi\| > 40°$
1704–1709	13 January 1981–14 July 1981	0.678	0.510	0.482
1734–1739	11 April 1983–21 July 1983	0.566	0.714	−0.437
1743–1748	12 December 1983–23 May 1984	0.332	0.600	−0.386

coefficients for the entire period of the uniform magnetic field measurements at the Wilcox Solar Observatory (since 1977) are shown in Figure 5.

It is seen from Table 2 and Figure 5 that, on the whole, the CGLB is closely related to the magnetic field strength. At the same time, this relation strongly depends on the solar latitude. In the sunspot formation zone (±30°) the correlation coefficient is rather high during the descending phase of the cycle and increases even more close to the minimum. The behaviour of the correlation coefficient is more complicated for the high-latitude zone (above 40°). It increases in the vicinity of maximum when the high-latitude field is relatively weak. Then, the correlation coefficient decreases and even changes sign as the minimum approaches. The cause of such a behaviour is not quite clear, but it is most likely due to different contribution of the local, large-scale and global fields at different phases of the cycle.

The regions where the CGLB is weak or strongly reduced are of particular interest. A long time ago, Waldmeier (1956, 1981) called such regions 'Loch in der Korona' (which means coronal hole in German), and later they were identified with the regions of reduced brightness in

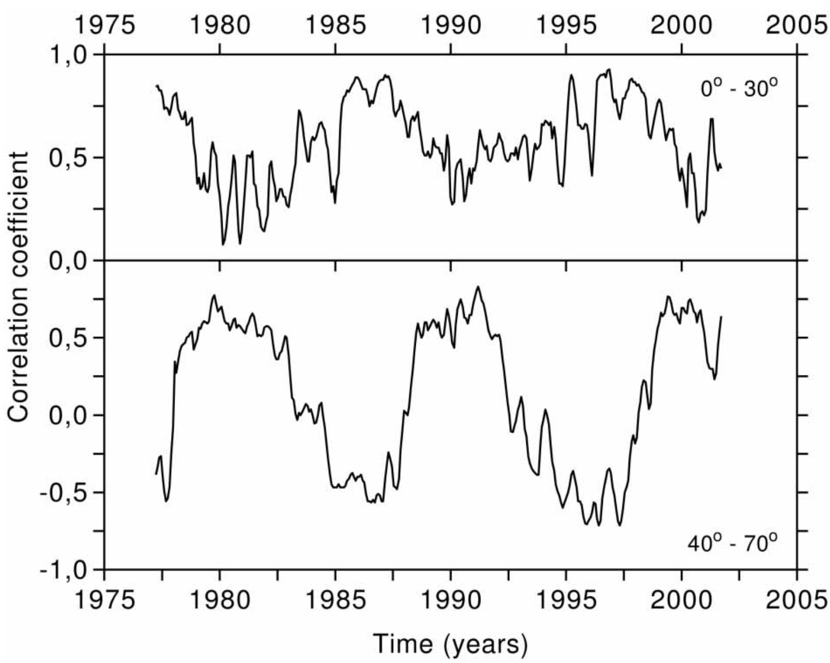

Figure 5. Time variation in the correlation between the magnetic field intensity and the CGLB for the set of space-coinciding points on the maps in the sunspot formation zone ±30° (upper plot) and in the zone outside the sunspots above ±40° (lower plot).

the extreme ultraviolet and X-ray emissions (Munro and Withbroe, 1972; Krieger *et al.*, 1973; Vaiana *et al.*, 1973).

Letfus *et al.* (1980) compared the regions of reduced CGLB with the positions of coronal holes as recorded by Skylab (Bohlin and Rubenstein, 1975) and good spatial correspondence of both formations was revealed. We present a similar comparison performed for two intervals of the Skylab flight when the well-known coronal hole CH1 was observed among others. The comparison clearly demonstrates that the very pronounced CH1 covers the area of considerably reduced CGLB (see the website at http://helios.izmiran.rssi.ru/hellab/Badalyan/green/).

We performed also a comparison of the CGLB and magnetic field strength with the coronal holes recorded on the Yohkoh soft X-ray images obtained via the Internet. A satisfactory correspondence of the regions of bright and weak coronas and the regions of enhanced and weak magnetic fields, respectively is noticeable (see the above-mentioned website).

Anyway, we are of opinion that the observed correlation between the coronal holes, decreased CGLB and magnetic field strength regions bears a statistical character only. In other words, the position of the open magnetic field lines is not the only factor determining the intensity of the green-line corona. One should, for example, take into account that the CGL intensity is measured along the line of sight at the solar limb. Therefore, any bright coronal regions, even rather distant from the plane of sky, may (owing to projection) overlap a possible faint region though situated close to that plane.

In spite of the above comments, the CGLB is clearly a good representation of the magnetic field strength and topology. Therefore, these data can be used to analyse the cyclic and structural variabilities of the solar activity governed, of course, by the variations in and evolution of the solar magnetic fields.

4 CONCLUSIONS

Evolution of the CGLB spatial distribution has been studied using the movie visualizing our coronal database (1943–2001). For the period 1977–2001 an extensive comparison with the coronal magnetic fields (as derived from the photospheric measurements) has been performed. The following results were obtained.

(1) Substantial changes in the spatial distribution of CGLB occur during relatively short periods of time close to the solar cycle reference points (originally derived from variations in other solar activity indices).
(2) The ALs have been reliably identified in the CGLB distribution, their lifetime being 1.5–3.0 years. As one AL weakens, another, distant by about 180°, is often seen to intensify (the so-called antipodal ALs).
(3) During high solar activity, two ALs are usually present on the Sun spaced by about 180°. This results in variations in solar activity (including the CGLB) with a period of 13–14 days. At the descending branch of the solar cycle a mutual penetration of the bright active regions from one to another solar hemisphere is commonly observed, creating the so-called ‘intermittent’ ALs. This means, in fact, that, during each solar rotation, one of the ALs is more pronounced in the northern hemisphere and the second (spaced by about 180°) is well developed in the southern hemisphere. At the minimum of the solar activity cycle, only one AL exists on the Sun.
(4) A deep genetic relationship is likely to exist between the space–time distribution of the CGLB and the evolution of the solar magnetic fields. Comparison of the synoptic charts constructed separately for the magnetic field strength and CGLB exhibits fairly good

agreement. This indicates that the CGLB distribution is considerably determined by the magnetic field strength at the corresponding height in the corona.

(5) It is found that the correlations between the CGLB and the magnetic field intensity are different in the sunspot formation and high-latitude zones. In the zone of $\pm 30°$, the correlation coefficient is always positive and increases towards the cycle minimum. Outside this zone, the correlation coefficient is positive at the maximum and negative at the minimum of the solar cycle. This may be due to existence of two different mechanisms of the corona heating.

The analysis performed in this paper demonstrates how highly informative the CGLB measurements are. The CGLB is one of a few solar activity indices that allow us to study the behaviour of solar activity at all heliographic latitudes by uniform data. The relation of the CGLB to the coronal magnetic fields makes it possible to go back in the investigation of these fields to periods for which the systematic measurements of the photospheric magnetic fields do not exist, that is to the early 1940s.

Of course, the intensity of the Fe XIV, 530.3 nm emission line merely indicates the mechanisms of the solar activity variations. Understandably, the magnetic field is a principal driver of these processes. Our analysis demonstrates that the green-line corona is deeply involved in the general scenario of the cyclic variations in solar activity. Thus, a long series of CGLB data can be used to extend the series of the existing magnetic field measurements backwards and/or to test any set of data obtained by other indirect methods. The CGLB database can also be effectively utilized to identify and study the phenomena important from the view point of their geoeffectivity, such as coronal holes, in periods prior to their direct space observations.

Acknowledgements

The authors greatly appreciate support by the Slovak Academy of Sciences (VEGA Grant 2/4013/24), the Russian Foundation for Basic Research (Grant 02-02-16199) and INTAS-2000-840. The Wilcox Solar Observatory staff is acknowledged for the data on solar magnetic fields obtained via the Internet.

References

Badalyan, O. G., and Kuklin, G. V. (1993) *Astron. Zh.* **70**, 856 (*Engl. transl. (1993) Astron. Rep.* **37**, 432).
Badalyan, O. G., and Kuklin, G. V. (2000) *Astron. Astrophys. Trans.* **18**, 839.
Badalyan, O. G., and Obridko, V. N. (2004a) *Astron. Zh.* **81**, 746 (*Engl. transl. (2004) Astron. Rep.* **48**, 678).
Badalyan, O. G., and Obridko, V. N., (2004b) In: A. V. Stepanov, E. E. Benevolenkaya and A. G. Kosovichev (eds), *Multi-Wavelength Investigations of Solar Activity*, IAU Symposium No. 223, Vol. 223 Cambridge University Press, Cambridge, p. 371.
Badalyan, O. G., Obridko, V. N., Kuklin G. V., and Sýkora, J. (2001a) *Issled. Geomagn., Aeron. Fiz. Solntsa* **113**, 33.
Badalyan, O. G., Obridko, V. N., and Sýkora, J. (2001b) *Solar Phys.* **199**, 421.
Benevolenskaya, E. E., Kosovichev, A. G., and Scherrer, P. H. (2000) In: *Proceedings of the American Astronomical Society*, SPD Meeting 31, Baton Range, LA, 26 February 2000, **32**, p. 815.
Berdyugina, S. V., and Usoskin, I. G. (2003) *Astron. Astrophys.* **405**, 1121.
Bohlin, J. D., and Rubenstein, D. M. (1975) *Report UAG-51*.
Bumba, V., Garcia, A., and Klvaňa, M. (2000) *Solar Phys.* **196**, 403.
Guhathakurta, M., Fisher, R. R., and Altrock, R. C. (1993) *Astrophys. J.* **414**, L145.
Guhathakurta, M., Fisher, R., and Strong, K. (1996) *Astrophys. J.* **471**, L69.
Krieger, A. S., Timothy, A. F., and Roelof, E. C. (1973) *Solar Phys.* **29**, 505.
Kuklin, G. V., and Obridko, V. N. (1995) *Izv. Russ Akad. Nauk, Ser. F12.* **59**, 12 (*Engl. transl. (1995) Bull. Russ. Acad. Sci., Phys.* **39**, 1120).
Kuklin, G. V., Obridko, V. N., and Vitinsky, Yu. I. (1990) In: R. J. Thompson, D. G. Cole, P. J. Wilkinson, M. A. Shea, D. Smart and G. Heckman (eds), *Solar–Terrestrial Predictions I*, Boulder, CO, p. 474.

Letfus, V., Kulčár, L., and Sýkora, J. (1980) In: M. Dryer and E. Tandberg-Hanssen (eds), *Solar and Interplanetary Dynamics*, Reidel, Dordrecht, p. 49.
Munro, R. H., and Withbroe, G. L. (1972), *Astrophys. J.* **176**, 511.
Neugebauer, M., Smith, E. J., Ruzmaikin, A. Feynman, J., and Vaughan, A. H. (2000) *J. Geophys. Res.* **105**, 2315.
Obridko, V. N., and Kuklin, G. V. (1994) In: J. Hruska, M. A. Shea, D. F. Smart and G. Heckman (eds), *Solar–Terrestrial Predictions IV*, Boulder, CO, p. 273.
Obridko, V. N., and Shelting, B. D. (2003) *Astron. Zh.* **80**, 1034 (*Engl. transl. (2003) Astron. Rep.* **47**, 953).
Stewart, G. A., and Bravo, S. (1996) *Adv. Space Res.* **17**, 217.
Sýkora, J. (1971) *Bull. Astron. Inst. Czech.* **22**, 12.
Sýkora, J. (1980) In: M. Dryer and E. Tandberg-Hanssen (eds), *Solar and Interplanetary Dynamics*, Reidel, Dordrecht, p. 87.
Sýkora, J. (1992) *Contrib. Astron. Obs. Skalnaté Pleso* **22**, 55.
Sýkora, J. (1994) *Adv. Space Res.* **14**, 73.
Sýkora, J., Badalyan, O. G., and Storini, M. (2002) *Adv. Space. Res.* **29**, 1975.
Sýkora J., and Rýbak, J. (2004) *Adv. Space. Res.* (in press).
Vaiana, G. S., Krieger, A. S., and Timothy A. F. (1973) *Solar Phys.* **32**, 81.
Vitinsky, Yu. I., Kopecky, M., and Kuklin, G. V. (1986a), *Statistics of Sunspot-Formation Activity*, Moscow, Nauka.
Vitinsky, Yu. I., Kuklin, G. V., and Obridko, V. N. (1986b) *Solnechnye Dannye* No.3, 53.
Waldmeier, M. (1956) *Z. Astrophys.* **38**, 219.
Waldmeier, M. (1981) *Solar Phys.* **70**, 251.
Wang, Y.-M., Sheeley, N. R., Jr, Hawley, S. H., Kraemer, J. R., Brueckner, G. E., Howard, R. A., Korendyke, C. M., Michels, D. J., Moulton, N. E., and Socker, D. G. (1997) *Astrophys. J.* **485**, 419.
Xanthakis, J., Mavromichalaki, H., Petropoulos, B., Tritakis, V., Paliatsos, A. G., Noens, J. C., and Pech, B. (1996) *Adv. Space Res.* **17**, 277.
Xanthakis, J., Petropoulos, B., Tritakis, V. P., Mavromichalaki, H., and Marmatsuri, L. (1991) *Adv. Space Res.* **11**, 169.